Contribution of phosphatidylserine to membrane surface charge and protein targeting during phagosome maturation

Tony Yeung,[1] Bryan Heit,[1] Jean-Francois Dubuisson,[2] Gregory D. Fairn,[1] Basil Chiu,[3] Robert Inman,[3] Andras Kapus,[4] Michele Swanson,[2] and Sergio Grinstein[1]

[1]Program in Cell Biology, The Hospital for Sick Children, Toronto, Ontario M5G 1X8, Canada
[2]Department of Microbiology and Immunology, University of Michigan Medical School, Ann Arbor, MI 48109
[3]Department of Medicine, Division of Rheumatology, University Health Network, University of Toronto, Toronto, Ontario M5T 2S8, Canada
[4]St. Michael's Hospital Research Institute, Toronto, Ontario M5B 1W8, Canada

During phagocytosis, the phosphoinositide content of the activated membrane decreases sharply, as does the associated surface charge, which attracts polycationic proteins. The cytosolic leaflet of the plasma membrane is enriched in phosphatidylserine (PS); however, a lack of suitable probes has precluded investigation of the fate of this phospholipid during phagocytosis. We used a recently developed fluorescent biosensor to monitor the distribution and dynamics of PS during phagosome formation and maturation. Unlike the polyphosphoinositides, PS persists on phagosomes after sealing even when other plasmalemmal components have been depleted. High PS levels are maintained through fusion with endosomes and lysosomes and suffice to attract cationic proteins like c-Src to maturing phagosomes. Phagocytic vacuoles containing the pathogens *Legionella pneumophila* and *Chlamydia trachomatis*, which divert maturation away from the endolysosomal pathway, are devoid of PS, have little surface charge, and fail to recruit c-Src. These findings highlight a function for PS in phagosome maturation and microbial killing.

Introduction

Macrophages and neutrophils eliminate apoptotic cells, foreign particles, and infectious organisms by phagocytosis (Niedergang and Chavrier, 2004; Swanson and Hoppe, 2004; Yeung et al., 2006a). The engulfment process is initiated by clustering of receptors on the surface of the phagocytic cell, which triggers a signaling cascade leading ultimately to the rearrangement of the actin cytoskeleton. Phosphoinositide metabolism is a key early event in phagocytosis; phosphatidylinositol (PI)-4,5-bisphosphate (PI[4,5]P_2), which is constitutively present in the membrane of unstimulated cells, accumulates transiently at the leading edge of pseudopods and subsequently disappears abruptly from the nascent phagosome. PI-3,4,5-trisphosphate (PI[3,4,5]P_3) is generated upon receptor engagement and vanishes shortly after phagosome closure (Botelho et al., 2000; Vieira et al., 2001). Because phosphoinositides are polyanionic, these biochemical changes are associated with a net reduction in the negative charge of the cytosolic surface of forming phagosomes (Yeung et al., 2006b). The surface charge in turn dictates the membrane association of proteins with polycationic clusters or polybasic domains (McLaughlin and Murray, 2005; Heo et al., 2006; Yeung et al., 2006b). As a result, the loss of surface negativity is thought to influence protein localization during phagocytosis (Yeung et al., 2006b).

After sealing, phagosomes undergo rapid and extensive remodeling of their membrane and contents. This process, called maturation, converts phagosomes into effective microbicidal and degradative organelles. Maturation entails further changes in the lipid composition of the phagosomal membrane, raising the possibility of additional fluctuations in surface charge and, consequently, in protein targeting. However, the major polyphosphoinositides are unlikely to contribute significantly to the charge of maturing phagosomes. PI[4,5]P_2 is undetectable when phagosomes seal and has not been reported to reappear during maturation,

Correspondence to Sergio Grinstein: sga@sickkids.ca

Abbreviations used in this paper: FRET, fluorescence resonance energy transfer; LUV, large unilamellar vesicle; mRFP, monomeric RFP; PA, phosphatidic acid; PC, phosphatidylcholine; PE, phosphatidylethanolamine; PI, phosphatidylinositol; PI[3]P, PI 3-phosphate; PI[3,4,5]P_3, PI-3,4,5-trisphosphate; PI[4,5]P_2, PI-4,5-bisphosphate; PS, phosphatidylserine; sRBC, sheep RBC.

The Rockefeller University Press $30.00
J. Cell Biol. Vol. 185 No. 5 917–928
www.jcb.org/cgi/doi/10.1083/jcb.200903020

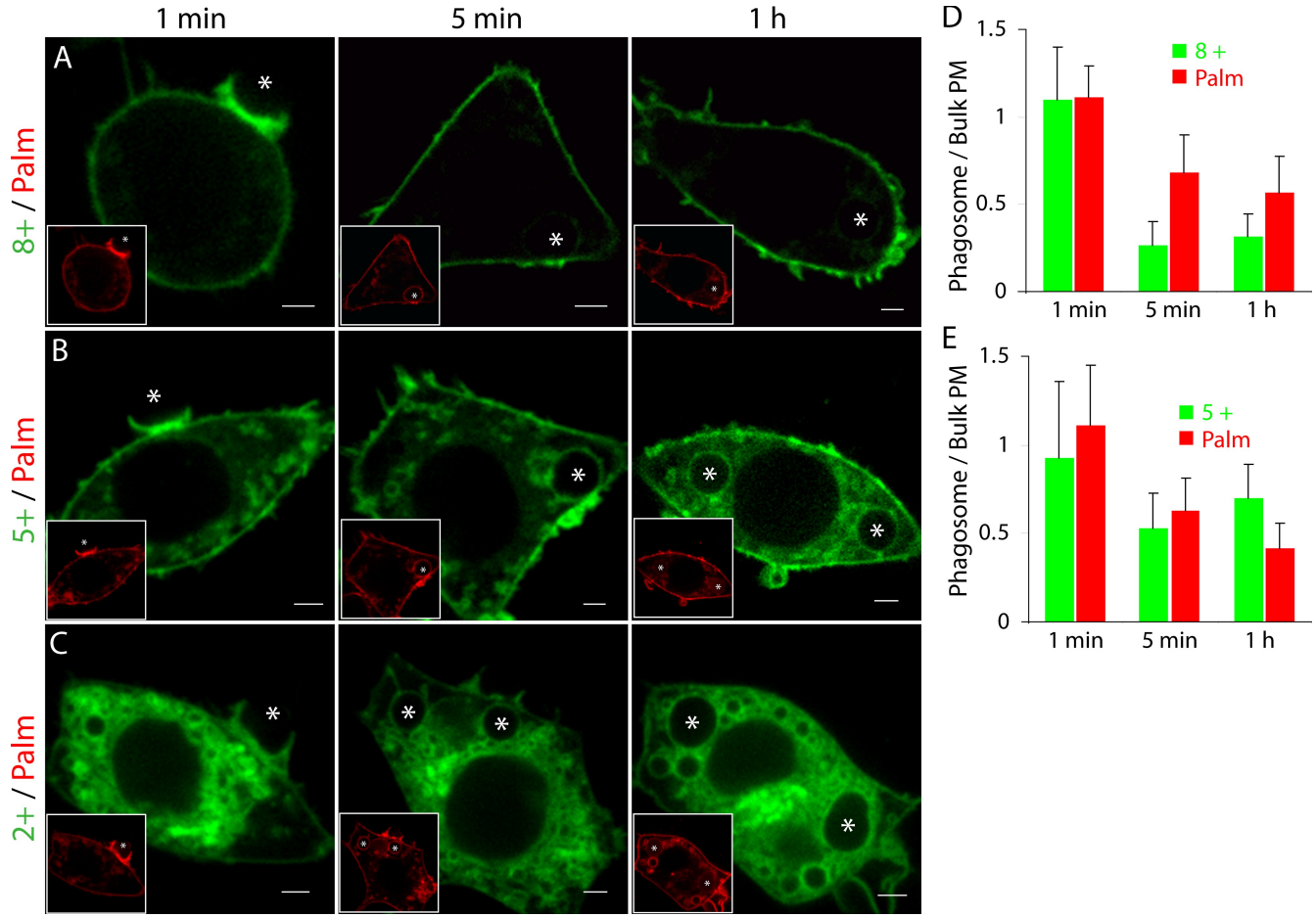

Figure 1. **Assessment of the surface charge of maturing phagosomes.** (A–C) RAW macrophages were cotransfected with mRFP-Palm, a farnesylated and dually palmitoylated construct modeled after the tail of H-Ras and fused to mRFP and either GFP-8+ (A), GFP-5+ (B), or GFP-2+ (C). The cells were exposed to IgG-opsonized sRBCs. Confocal images were acquired 1 min, 5 min, or 1 h after initiation of phagocytosis. GFP fluorescence of the surface charge probes is shown in the main panels, whereas mRFP-Palm is shown in the insets. The asterisks denote the position of the sRBCs. Images in A–C are representative of at least 30 cells from two similar experiments. (D and E) Quantification of the fluorescence intensity of GFP-8+ and GFP-5+ (green bars in D and E, respectively) and mRFP-Palm (red bars) at the specified stage of maturation. Results are presented as the ratio of fluorescence intensity at the phagosome to that in the bulk, unengaged plasma membrane (PM). Data in D and E are means ± SD calculated from 10 cells from a representative experiment. Bars, 2 µm.

and PI[3,4,5]P_3 disappears from nascent phagosomes within 1 min of sealing (Marshall et al., 2001). In contrast, little is known about phosphatidylserine (PS), the most abundant anionic phospholipid (Vance and Steenbergen, 2005). Because it is asymmetrically distributed, PS is thought to be a major contributor to the surface charge of the inner aspect of the plasmalemma (Leventis and Silvius, 1998). Nevertheless, the fate of this lipid during phagosome formation and maturation has not been studied in any detail due in all likelihood to the lack of suitable means of detection.

We recently designed a genetically encoded biosensor for PS that can be used to monitor the distribution and dynamics of the phospholipid in intact, live cells (Yeung et al., 2008). The probe consists of a discoidin-type C2 domain, which binds selectively to PS, attached to a green or red fluorescent protein. In this study, we used such chimeras to examine the fate of PS during the formation and maturation of phagosomes. In addition, we monitored the surface charge of maturing phagosomes and compared the properties of vacuoles containing inert particles with those containing pathogens that survive intracellularly by eluding the microbicidal machinery of phagocytes.

Results

Assessment of surface charge during phagosome maturation

The surface charge of biological membranes can be monitored in situ using genetically encoded fluorescent probes (Yeung et al., 2006b). These consist of two targeting determinants: a hydrophobic moiety that guides the probe to membranes and a polycationic motif that dictates preferential distribution to the most negatively charged surfaces. By linking these determinants to fluorescent proteins, the charge of membranes can be monitored in live cells by confocal microscopy. As we reported earlier (Yeung et al., 2006b), a highly cationic probe (containing eight positive charges and a farnesyl anchor, termed hereafter 8+) distributes almost exclusively to the inner aspect of the plasma membrane of resting macrophages, accumulates briefly at sites of particle engagement, and dissociates precipitously from phagosomes as they seal (Fig. 1 A). Similar results were obtained using IgG-opsonized red cells (Fig. 1, A and D) or latex beads (Fig. S1, A and D) as phagocytic targets. The 8+ probe

did not reassociate with the phagosomes as they matured; compared with the plasma membrane, only a small fraction of the probe was detectable on phagosomes after 1 h of their formation (Fig. 1, A and D; and Fig. S1, A and D). Although maturing phagosomes undergo both fusion with other organelles and concomitant fission, the rapid detachment of the probe cannot be attributed to generalized exchange of lipids between the phagosome and other intracellular compartments. This was concluded by comparison with two other probes that are associated with the plasma membrane. As shown in Fig. 1 and in Fig. S1, a dually acylated and farnesylated probe tagged with monomeric RFP (mRFP; mRFP-Palm) is partially lost from the phagosomes as they begin to mature, but the rate and extent of loss were considerably lower than that of the 8+ probe and likely insufficient to account for the nearly complete loss of the 8+ probe (Fig. 1 A, middle). Similar results were obtained using a different probe, GT46, which unlike mRFP-Palm, is thought to be excluded from rafts (Pralle et al., 2000). GT46 is a transmembrane chimeric protein consisting of the signal sequence from rabbit lactase fused to the transmembrane domain of the human low density lipoprotein receptor and containing the intracellular domain of CD46. As shown in Fig. S2 A and Video 1, GT46 prominently labeled the forming phagosome and was retained for >6 min after the phagosome had sealed. Like the 8+ probe, which is lysine rich, another prenylated 8+ probe containing eight tandem arginines (R-pre) was largely depleted from the formed phagosome after 3–5 min (Fig. S2, B and C; and Video 1). Jointly, these observations indicate that the loss of the 8+ probes cannot solely be attributed to extensive remodeling of the phagosomal membrane through fusion/fission with other organelles.

To test whether the charge of the 8+ probe dictates its response during phagocytosis, we followed the distribution of a probe with its net positive charge reduced to 2+ by mutagenesis. The distribution of the probe (2+) in resting cells was grossly altered with extensive labeling of endomembranes in addition to the plasmalemma (Fig. 1 C). More importantly, during maturation, the phagosomes lost only a small fraction of the label. Because both the 8+ and 2+ are farnesylated, these observations indicate that the pronounced loss of the 8+ probe from phagosomes was not a result of altered hydrophobic interactions and is instead attributable to a drop in the surface charge.

The extent to which the phagosomal surface potential was reduced was assessed in more detail using a probe with a net charge of 5+. This probe was shown earlier to associate with the plasma membrane but also with a subpopulation of endomembranes that have an intermediary degree of negative surface charge (Fig. 1 B and Fig. S1 B; Yeung et al., 2008). Interestingly, both the nascent and mature phagosome were labeled by this probe (Fig. 1, B and E), suggesting that the phagosomal membrane was not totally devoid of charge. Of note, the loss of the acylated (Palm) membrane marker was greater than that of the 5+ probe after 1 h (Fig. 1 E), suggesting that the surface charge is conferred by constituents acquired during maturation and not solely by those retained from the original surface membrane. Indeed, the transmembrane protein GT46 that demarcated the forming and early phagosome (Fig. S2 D) was virtually absent from phagosomes that underwent maturation for 1 h (Fig. S2 E), implying that extensive remodeling of the phagosomal membrane had occurred by this time. This observation suggests that the charge associated with the phagosome after 1 h is dictated primarily by components acquired in the course of maturation.

PI 3-phosphate (PI[3]P) is not required for charge maintenance on the phagosome

We next examined the mechanisms contributing to the charge of the maturing phagosome. Because phosphoinositides were found to be important for the plasmalemmal targeting of proteins with polybasic domains (Heo et al., 2006), we tested whether they contribute also to charge maintenance during phagosome maturation. Although neither PI[4,5]P_2 nor PI[3,4,5]P_3 have been detected in maturing phagosomes, PI[3]P is evident during the first 10–15 min of the maturation process, disappearing thereafter (Fig. 2, A [middle] and D; Vieira et al., 2001). To assess whether PI[3]P is necessary for the maintenance of charge on maturing phagosomes, macrophages were treated with the PI 3-kinase inhibitor wortmannin after multiple particles had been ingested. As expected, the inhibitor rapidly terminated the synthesis of PI[3]P, as judged by the dissociation of the 2FYVE (Fab1/YOTB/Vac1/EEA1) construct that binds specifically to this inositide (Fig. 2, B [middle] and D; Gillooly et al., 2001). However, the association of the 5+ probe persisted (Fig. 2, B and C), implying that PI[3]P is not the major determinant of the negative surface charge of maturing phagosomes.

The anionic lipid PS is present in the phagosomal membrane

Because phosphoinositides failed to explain the association of the polycationic probe with phagosomes, we turned our attention to PS, the most abundant anionic phospholipid. We had earlier attempted to detect PS in phagosomes using annexin-V and an anti-PS antibody but obtained negative results (Yeung et al., 2006b). However, these results must be interpreted with great caution for multiple reasons. First, neither annexin-V nor anti-PS antibodies can be used in live cells, and fixation followed by permeabilization is required. In addition, annexin binding to PS requires elevation of calcium to concentrations three to four orders of magnitude greater than the physiological cytosolic level. These procedures are themselves liable to alter the lipid distribution. Furthermore, despite being used extensively to label PS, neither annexin-V nor anti-PS antibodies are specific for this lipid. This is illustrated in Fig. S3, where the binding of these reagents to various lipids was tested in vitro. Although the anti-PS antibody bound negligibly to phosphatidylcholine (PC), phosphatidylethanolamine (PE), and PI[4,5]P_2, it did recognize phosphatidic acid (PA) and PI in addition to PS (Fig. S3 A). Annexin-V was even less specific, binding PA and phosphatidylglycerol to a similar extent as PS and PI[4,5]P_2 to a lower degree (Fig. S3 B). These findings are consistent with the previous study of Raynal and Pollard (1994).

We therefore reanalyzed the distribution of PS during maturation using as a probe the C2 domain of lactadherin, which was shown earlier to be highly specific (Andersen et al., 2000; Yeung et al., 2008). Indeed, discoidin family C2 domains are stereospecific, capable of differentiating between the L- and

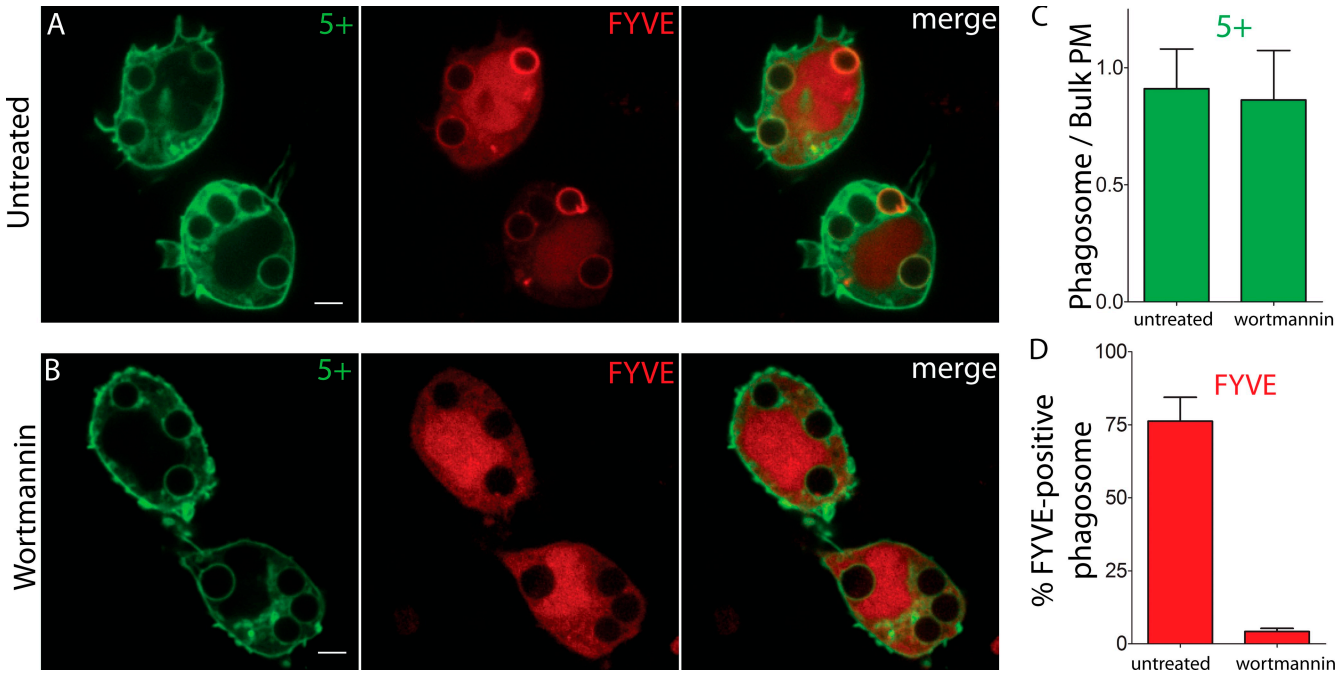

Figure 2. **Depletion of PI[3]P fails to alter the phagosomal surface charge.** (A and B) RAW macrophages were cotransfected with a construct consisting of two tandem PI[3]P-binding FYVE domains of EEA1 fused to mRFP (2FYVE-mRFP; red) and the GFP-5+ probe (green). (A) The cells were exposed to opsonized sRBCs, and confocal images were acquired after 15–20 min. (B) The cells were treated with wortmannin for an additional 15 min, and additional images were acquired. (C and D) Quantification of the ratio of fluorescence intensity of GFP-5+ on the phagosome versus the bulk plasma membrane (C) and the percentage of 2FYVE-mRFP–positive phagosomes (D) before and after wortmannin treatment. PM, plasma membrane. Images are representative of 20 fields from two similar independent experiments; quantification was performed on those same images. Data are means ± SEM quantified from at least 15 phagosomes from two experiments. Bars, 2 µm.

D-stereoisomers of phosphoserine (Gilbert and Drinkwater, 1993; Shi et al., 2004). A GFP-tagged form of the C2 domain of lactadherin (GFP-Lact-C2) was expressed in macrophages, and its distribution was analyzed during the course of phagosome formation and maturation using spinning-disc confocal microscopy. As shown in Fig. 3 and Fig. S4, GFP-Lact-C2 is found at the plasma membrane as well as in intracellular organelles that were identified earlier as components of the endocytic pathway (Yeung et al., 2008). During the course of phagocytosis, GFP-Lact-C2 was associated with the phagosomal membrane for at least 1 h (Fig. 3 C). The levels of PS, as estimated by the density of GFP-Lact-C2 per unit area, were similar to those found in the plasma membrane (Fig. 3 D and Video 2).

Comparison of the density of GFP-Lact-C2 with that of the membrane markers mRFP-Palm and GT46 provides clues of the source of the PS. At the earliest times, a transient accumulation of GFP-Lact-C2 at the phagosomal cup was paralleled by accumulation of the Palm probe (similar observations were made for GT46; Fig. 3, A and D). This probably reflects the increased density of membranes at sites of engulfment as a result of convolution or recycling of the plasma membrane. Shortly after sealing (Fig. 3, B and D [5-min data]; and Fig. S2 D), the density of all the probes is comparable with that in the plasmalemma, suggesting that PS is neither enriched nor depleted during invagination of the phagosomal membrane. However, after 1 h, the density of both Palm and GT46 decreases markedly (Fig. 3, B and C; and Fig. S2 E) as the phagosome matures and the remnants of the plasma membrane are gradually depleted. Remarkably, the density of GFP-Lact-C2 remains nearly constant from 5 min to 1 h. This implies that either (a) components of the plasma membrane are removed selectively with PS persisting longer than the microdomains that harbor the Palm and GT46 probes or (b) PS is delivered from other sources, as the PS originally present in the invaginated plasmalemma is removed. We favor the latter interpretation because endosomes and lysosomes, which are known to fuse with the maturing phagosome, are well endowed with PS (Yeung et al., 2008). Indeed, dynamic visualization of the maturation process revealed active and continuous interaction of PS-enriched vesicles with the maturing phagosome (Video 2).

To more directly confirm the occurrence of fusion of internal organelles bearing PS with the maturing phagosomes, we labeled endocytic membranes by pulsing the cells for 15 min with the membrane-associated impermeant dye FM4-64 (Fig. S4, A–C). The labeled membranes overlapped extensively with the PS endomembrane compartment (the Manders colocalization coefficient for FM4-64/Lact-C2 was 0.933). During the course of maturation, phagosomes acquired FM4-64 (Fig. S4 B, arrows), which is indicative of fusion with endocytic membranes. Because the overwhelming majority of the FM4-64–labeled structures were also labeled by Lact-C2, such fusion must have delivered PS to the phagosomal membrane. Indeed, while acquiring videos, we were able to capture fusion events of phagosomes with structures labeled with both FM4-64 and Lact-C2 (Fig. S4 C).

Despite the ongoing delivery of PS-containing vesicles to the phagosome, neither its surface area nor its PS content

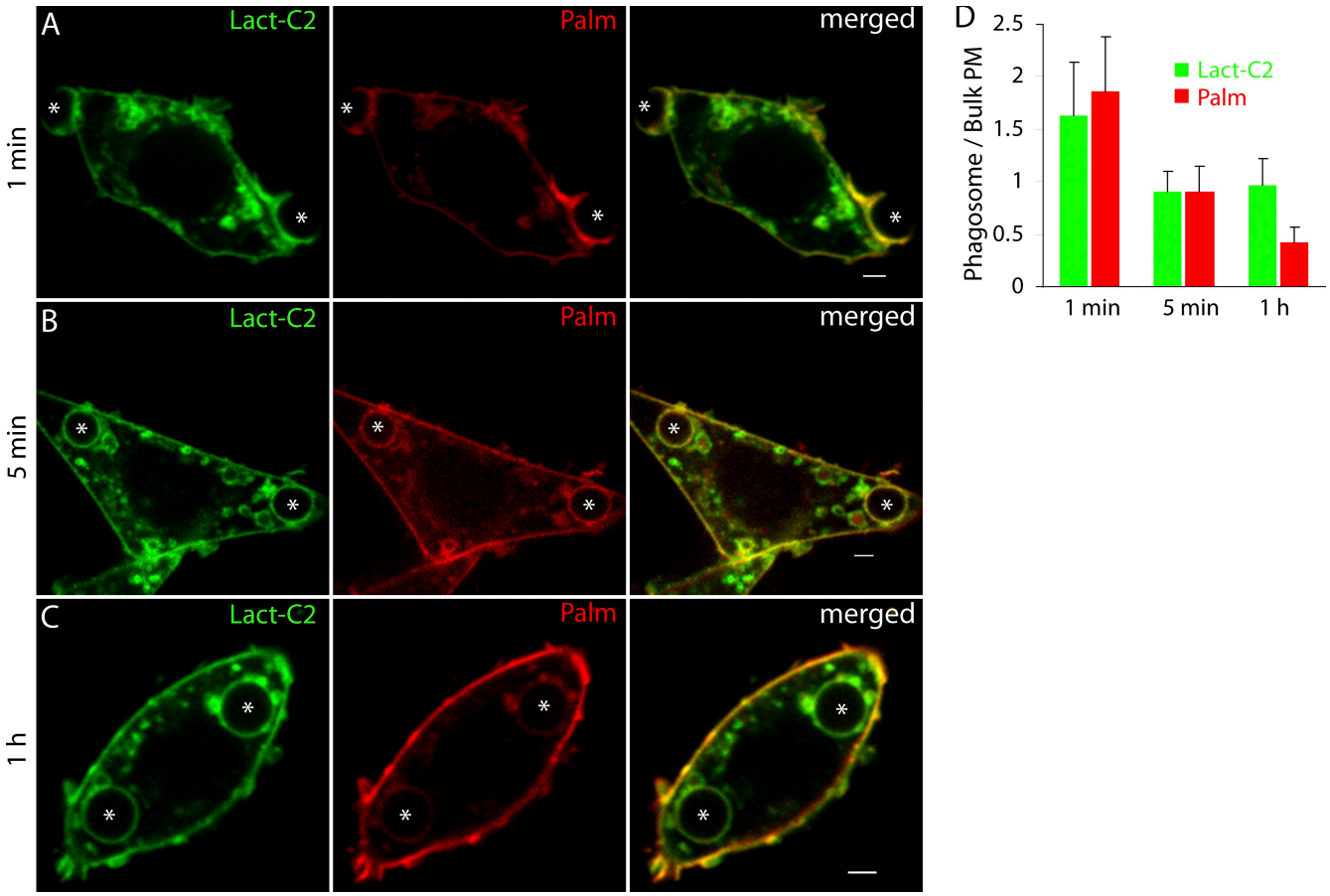

Figure 3. **Distribution of PS during phagosome formation and maturation.** (A–C) RAW macrophages cotransfected with mRFP-Palm and the PS biosensor GFP-Lact-C2. The cells were exposed to IgG-opsonized sRBC. Confocal images were acquired 1 min (A), 5 min (B), or 1 h (C) after initiation of phagocytosis. The GFP fluorescence of the PS biosensor is shown in the left column, mRFP-Palm is shown in the middle, and the two channels were merged in the right column. Images in A–C are representative of 30 cells from two independent experiments. (D) Quantification of the fluorescence intensity of GFP-Lact-C2 (green bars) and mRFP-Palm (red bars) at the specified stage of maturation. The results are presented as the ratio of fluorescence intensity of the phagosome to that in the bulk, unengaged plasma membrane (PM). Asterisks indicate location of sRBCs. Data are means ± SD of 10 cells from a typical experiment. Bars, 2 μm.

increases visibly during maturation. This is probably attributable to the concomitant removal of membranous material, which in all likelihood includes PS. This notion was verified by labeling the membrane at the time of phagocytosis with cholera toxin subunit B. As shown in Fig. S4 (D–F), tubules (arrows) colabeled by Lact-C2 and cholera toxin were observed to extend from the phagosome and eventually undergo fission. Together, these observations indicate that, although its overall concentration is nearly constant during maturation, PS is continuously delivered to and removed from phagosomes during the process.

We also studied the fate of PS in phagosomes formed by ingestion of latex beads. In this case, PS similarly persisted in the phagosomes, although at a somewhat reduced level (Fig. S1, F–I). Of note, the association of the 5+ probe was also reduced in these phagosomes (Fig. S1 B). The mechanisms underlying the difference between phagosomes that contain red blood cells versus latex beads and other synthetic particles is unclear (Oh and Swanson, 1996), but the parallel behavior of the GFP-Lact-C2 and 5+ probes in both cases supports the notion that PS is an important determinant of the charge of maturing phagosomes.

Intracellular pathogens modify the PS content of phagosomes

We inferred from the previous experiments that PS is delivered to the phagosome during maturation through fusion with compartments of the endocytic pathway. To test this hypothesis, we exploited as phagocytic targets pathogenic microorganisms that, while entering plasma membrane–derived vacuoles as do inert particles, subsequently coopt the cellular machinery to divert traffic away from the endolysosomal pathway. *Legionella pneumophila* is one such intracellular pathogen. After entry into the host cell, *L. pneumophila* propagates in a unique compartment derived largely from the endoplasmic reticulum (Swanson and Isberg, 1995). This phenotype was readily replicated in the RAW macrophages used in this study. As illustrated in Fig. 4 A, 4–6 h after infection, *L. pneumophila* occupies a vacuole enriched in sec61α, an ER marker. Importantly, the *L. pneumophila*–containing vacuole was devoid of PS, as indicated by the absence of mRFP-Lact-C2 (Fig. 4, B and D). The paucity of Lact-C2 was likely the result of bacterial effectors that are delivered to the host cell where they actively divert membrane traffic (Shin and Roy, 2008). This could be demonstrated by killing the bacteria before phagocytosis.

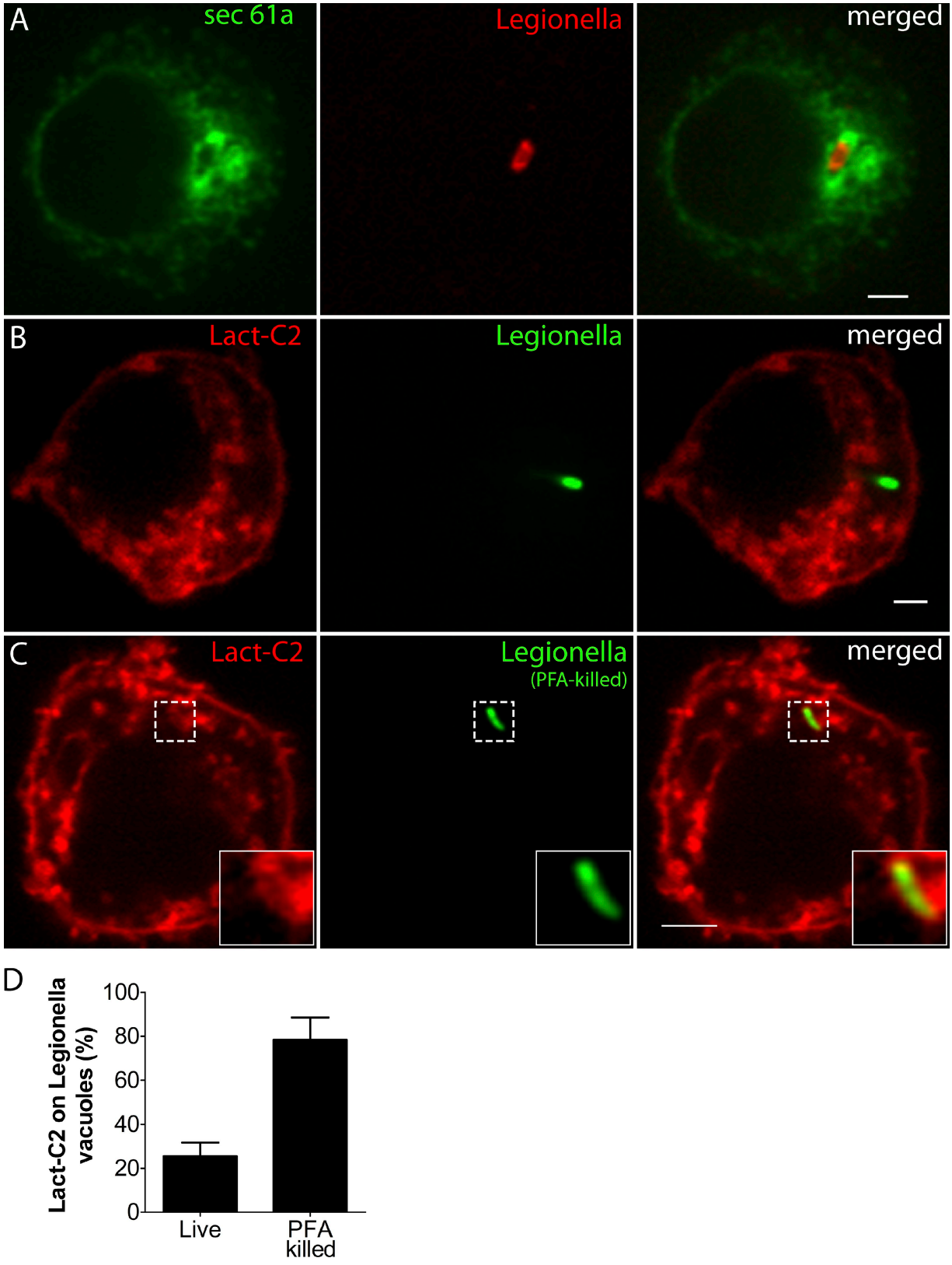

Figure 4. ***L. pneumophila*–containing vacuoles are devoid of PS.** (A) RAW macrophages transfected with sec61α-GFP were infected with *L. pneumophila* for 2 h, washed, and further incubated for 2–4 h. Cells were fixed and permeabilized with cold methanol, and the internalized bacteria were stained with an anti–*L. pneumophila* antibody followed by a Cy3-conjugated secondary antibody. (B and C) RAW macrophages transfected with the PS biosensor mRFP-Lact-C2 were infected with live (B) or were allowed to phagocytose PFA-treated (C) *L. pneumophila* expressing GFP-*fla*A for 2 h. The RAW macrophages were washed and further incubated for 2–4 h. Insets in C show a magnification of the boxed areas showing a Lact-C2–positive *L. pneumophila*–containing vacuole. Images in A–C are representative of 30 cells from two similar experiments. (D) Quantification of the percentage of vacuoles containing either live or PFA-killed *L. pneumophila* that bound Lact-C2. Data are means ± SEM quantified from >30 phagosomes. Bars, 2 µm.

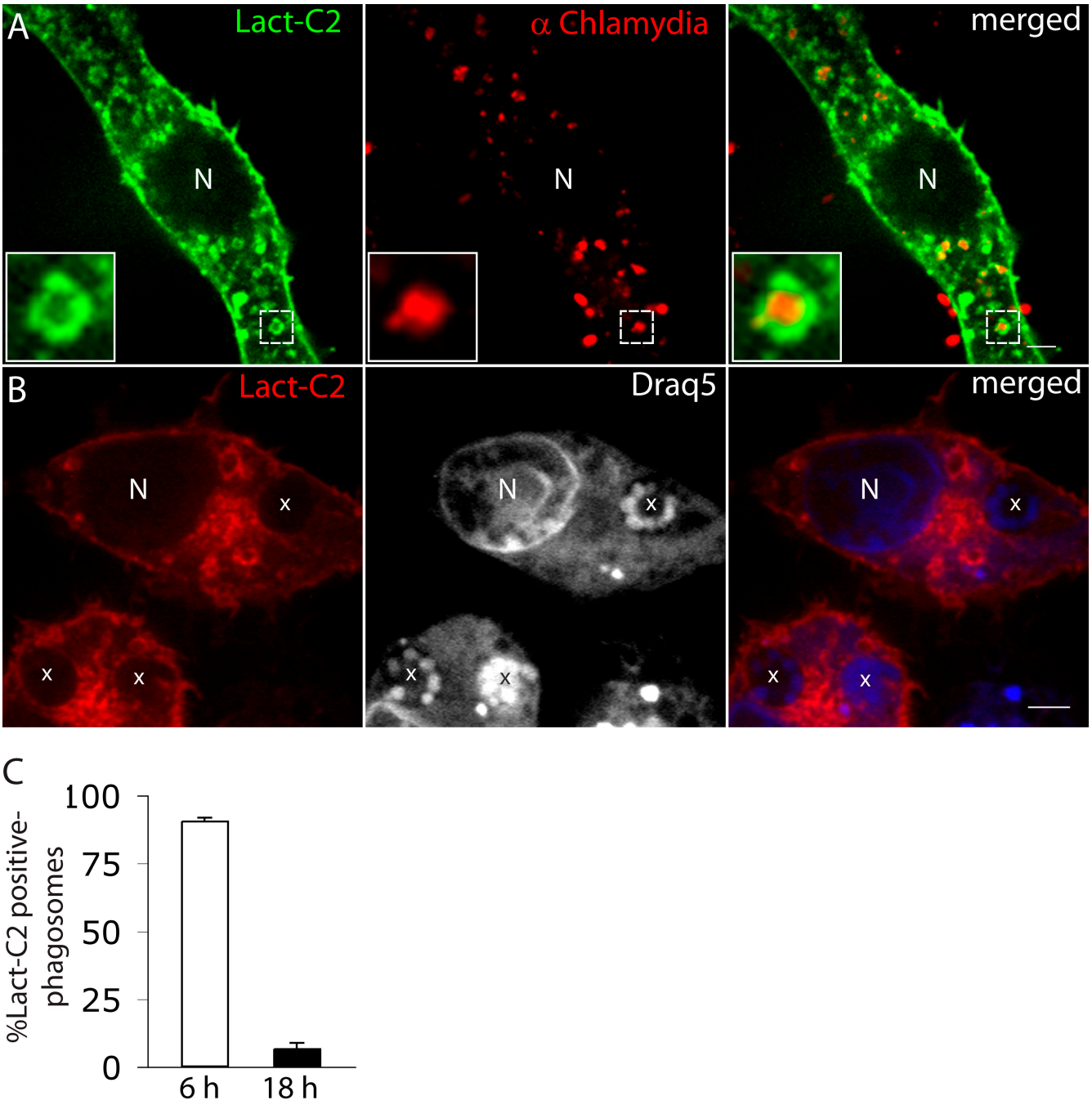

Figure 5. **Assessment of the presence of PS in *C. trachomatis* inclusion vacuoles.** (A) RAW macrophages transfected with GFP-Lact-C2 were infected with *C. trachomatis* elementary bodies for 6 h. Cells were fixed and permeabilized with cold methanol, and the internalized bacteria were stained with polyclonal anti–*C. trachomatis* antibodies followed by Cy3-conjugated secondary antibody. Insets highlight the typical vacuole marked by the boxed regions. (B) RAW macrophages transfected with mRFP-Lact-C2 were infected with *C. trachomatis* elementary bodies for 18 h. Cells were incubated with the DNA stain Draq5 to identify the *C. trachomatis* invasion vacuoles (x). N indicates the location of the macrophage nucleus. Images are representative of 30 cells from three similar experiments. (C) Quantification of the percentage of *C. trachomatis* inclusion vacuoles that bound Lact-C2 at 6 and 18 h. Data are means ± SEM quantified from at least 50 phagosomes from two experiments. Bars, 2 µm.

When macrophages were allowed to phagocytose PFA-fixed *L. pneumophila*, the resulting phagosomes matured normally, acquiring PS (Fig. 4, C and D).

C. trachomatis is another intracellular pathogen that evades the endolysosomal pathway. The microorganisms initially enter the conventional endocytic pathway but subsequently deploy effectors that reroute the pathogen to a unique compartment often found in the proximity of the Golgi apparatus from where it is thought to draw lipids (Salcedo and Holden, 2005; Brumell and Scidmore, 2007). We therefore analyzed the PS content of the *C. trachomatis* inclusion vacuole at early and late times after infection. 4–6 h after infection, most vacuoles contained single bacteria, which were detectable by immunostaining. At this early stage, the vacuole surrounding *C. trachomatis* was prominently

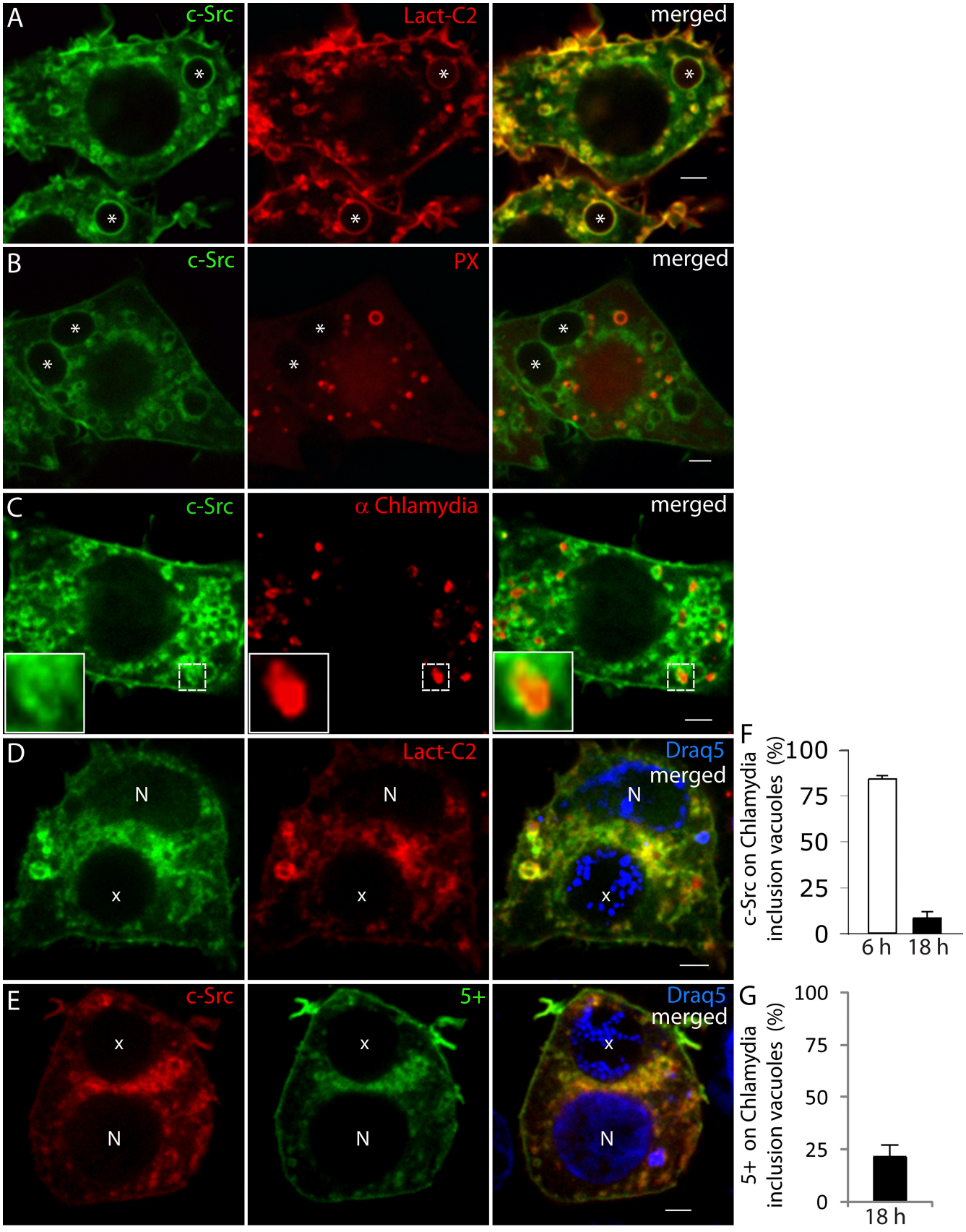

Figure 6. **PS is required for the targeting of Src to the phagosome.** (A and B) RAW macrophages cotransfected with c-Src–GFP (green) and the PS biosensor mRFP-Lact-C2 (red; A) or cotransfected with c-Src–GFP (green) and the PI[3]P biosensor mRFP-PX (red; B). The cells were exposed to IgG-opsonized sRBCs, and confocal images were acquired 1 h after initiation of phagocytosis. Asterisks denote phagosomes. (C–E) RAW macrophages transfected with

decorated by the Lact-C2 probe (Fig. 5, A and C), indicating that it contained a substantial level of PS. However, after 18 h, *C. trachomatis* resided and proliferated within an unusually large membrane-bound vacuole. As shown in Fig. 5 (B and C) and Fig. 6 D, although surrounded by Lact-C2–positive structures, *C. trachomatis* inclusion vacuoles were themselves devoid of Lact-C2. Thus, the vacuoles surrounding bacteria that evade the endolysosomal system lack PS. These observations add credence to the notion that in normal phagosomes, PS levels are maintained by dynamic interactions with endosomes and lysosomes.

PS contributes to the phagosomal targeting of signaling proteins with cationic motifs

The negative charge conferred to phagosomes by PS was shown in Fig. 1 B to correlate and most likely promote the recruitment of probes with an intermediate surface charge (e.g., 5+). By extension, it can be expected that the negative surface charge of maturing phagosomes would similarly induce the recruitment of moderately cationic signaling molecules. One possible target is the tyrosine kinase Src, which is important for phagocytosis and phagolysosome fusion (Majeed et al., 2001; Peyron et al., 2001). Like our intermediate surface charge probes, Src possesses a cationic motif of net charge 5+ in the vicinity of a hydrophobic (myristoyl) tail located at its N terminus. As shown in Fig. 6 A, Src was targeted to the plasma membrane and to internal organelles in macrophages. Although phosphoinositides likely contribute to the electrostatic partitioning of Src to the plasma membrane, they are not important determinants of its association with endomembrane compartments. Neither PI[4,5]P_2 nor PI[3,4,5]P_3 are found in endomembranes, and, as shown in Fig. 6 B, PI[3]P in endosomes does not colocalize well with intracellular Src. Instead, the distribution of Src overlaps extensively with that of PS (Fig. 6 A).

The contribution of PS to the endomembrane distribution of Src is further illustrated by experiments using *C. trachomatis* as the phagocytic target. As shown in Fig. 5, *C. trachomatis* inclusion vacuoles contain PS at early but not late stages. The same pattern was noted for Src, which was present on vacuoles 4–6 h after infection (Fig. 6, C and F) but not after 18 h (Fig. 6, D and G). The absence of Src from the late *C. trachomatis* vacuoles is in all likelihood the result of their reduced surface charge, as the vacuoles also fail to bind the 5+ probe (Fig. 6, E and G).

Discussion

We previously reported that the surface charge of the region of the membrane engaged in phagocytosis was altered drastically during the course of particle engulfment (Yeung et al., 2006b). Specifically, we found that highly cationic (8+) probes detached from the nascent phagosome, indicating a decrease in the surface charge. The collapse of charge was postulated to be the result of the metabolism or redistribution of phosphoinositides and/or PS during phagocytosis. In particular, the tetravalent PI[4,5]P_2, which is estimated to constitute 2–5% of the lipid of the inner leaflet of the plasma membrane, disappears from forming phagosomes with kinetics that mirror closely the fate of the 8+ surface charge probes (Botelho et al., 2000; Yeung et al., 2006b). However, the fate of PS could not be determined unequivocally as a result of limitations of the reagents available at the time (see Results; Fig. S3). The recent development of a genetically encoded PS biosensor allowed us the unprecedented opportunity to monitor in vivo the fate of this lipid during the course of phagosome formation and maturation. Using this probe, we found that, unlike PI[4,5]P_2, PS persists for extended periods on the membrane of formed, maturing phagosomes. This observation is consistent with an earlier study that PS constitutes ∼9% of the total lipid content of isolated phagosomes (Desjardins et al., 1994). A fraction of the PS originally present in nascent phagosomes most likely derives from the plasma membrane, which invaginates to provide the bulk of the membrane of early phagosomes. This is confirmed by the presence in early phagosomes of a variety of plasmalemmal markers regardless of whether they are diacylated, transmembrane, or GPI-linked proteins (Fig. 1 and Fig. S2; Yeung et al., 2006b). However, PS persists in the membrane of maturing phagosomes even after the plasmalemmal markers have been depleted by fusion and selective fission events (Fig. S4). Previously, we reported that early and late endosomes as well as lysosomes contain PS in their cytosolic-facing monolayer (Yeung et al., 2008). In this study, we observed that PS-positive endosomes were continuously being delivered to the phagosomes as they mature (Fig. S4 and Video 2). Based on these results, we concluded that the PS content of the phagosome is dictated by the maturation sequence and is liable to be affected when the process is subverted by pathogens.

Although PI[4,5]P_2 is eliminated from maturing phagosomes, the persistence of PS raised the intriguing possibility that the phagosome may not be totally devoid of charge. Unlike the highly cationic 8+ probes, which are almost quantitatively bound by the highly negative plasmalemma, probes of intermediate charge (e.g., 5+) are not fully partitioned to the plasma membrane and permit the visualization of organelles with lower yet significant charge. Using GFP-5+, we found that the cytosolic leaflet of phagosomes is indeed negatively charged throughout the maturation process. Phosphoinositides do not contribute significantly to this charge; PI[4,5]P_2 is not detectable in formed phagosomes, and PI[3,4,5]P_3 persists for ≤1 min after sealing. PI[3]P, which is formed subsequently, and its derivative, PI[3,5]P_2, are not essential to confer charge to maturing phagosomes, which bind comparable amounts of the 5+ probe both before and after treatment with inhibitors of the class III PI 3-kinase (Fig. 2). These findings

c-Src and cotransfected with mRFP-Lact-C2 (D) or GFP-5+ (E) were infected with *C. trachomatis* elementary bodies for 4 (C) or 18 h (D and E). Cells in C were stained with anti–*C. trachomatis* antibodies, whereas those in D and E were incubated with the DNA stain Draq5 to identify the *C. trachomatis* invasion vacuoles (x). N indicates the location of the macrophage nucleus. Insets show a magnified *C. trachomatis* elementary body at 4 h as marked by the box. Images in A–E are representative of at least 30 cells from two similar experiments. (F) Quantification of the percentage of *C. trachomatis* inclusion vacuoles that bound c-Src at 6 and 18 h. (G) Quantification of the percentage of *C. trachomatis* inclusion vacuoles that bound the 5+ probe. Data in F and G are means ± SEM quantified from at least 35 phagosomes from two similar experiments. Bars, 2 µm.

are most likely explained by the postulate that PS is the primary determinant of the phagosomal charge. However, the possible contribution of other anionic lipids such as PA and lysobis-PA should not be neglected, pending the development of suitable probes to detect these species.

Although the correlation between phagosomal PS and surface charge is strong, it is difficult to establish unambiguously the causal relationship between these parameters. Mammalian cells cannot be fully depleted of PS by either genetic deletion of the PS synthase isoforms or by pharmacological means. However, in the case of phagosomes, the subversion of the maturation process by certain intracellular pathogens provides an opportunity to test the role of PS. To avert killing, virulent microorganisms like *L. pneumophila* and *C. trachomatis* coopt the machinery of host cells to divert maturation away from the endolysosomal pathway. As shown in Figs. 4–6, the mature pathogen-containing vacuoles are devoid of detectable PS and, importantly, are also devoid of either the 5+ probe or the similarly charged Src. These findings further support the notion that PS is a key contributor to the charge of phagosomes and invasion vacuoles.

Regardless of its contribution to the surface charge, the presence of PS in phagosomes is expected to have important functional consequences. In this regard, we have preliminary evidence that yeast that are deficient in the PS synthase gene (*cho1*), and therefore lack PS, have defective vacuolar acidification (Fig. S5 A), and their endocytic pathway has abnormal appearance and traffic as revealed by FM4-64 pulse-chase analyses (Fig. S5, B and C). Although the mechanisms accounting for the aberrant phenotype remain to be explored, they likely include the failed targeting of PS-binding proteins.

A sizable number of proteins contain C2 domains that bind PS with varying degrees of selectivity. Several of these, such as protein kinase C and phospholipase C isoforms, are engaged in signal transduction, whereas others, like the synaptotagmins, control membrane fusion events. Both phenomena are central to the maturation of endosomes and phagosomes. Similarly, regardless of whether PS is its main determinant, the negative charge of phagosomes will serve to target proteins with polycationic clusters or polybasic domains, particularly those that also contain hydrophobic moieties. Indeed, our work reveals that the phagosomal distribution of one such molecule, the tyrosine kinase c-Src, shows strong correlation with the presence of PS in the phagosomal membrane. Similarly, PS may be a critical determinant in the distribution of small GTPases of the Rab and Rho superfamilies, which have been shown to be guided electrostatically to cellular membranes (Heo et al., 2006) and are important participants in phagosome formation and maturation.

In summary, we found that PS enters phagosomes as the plasma membrane invaginates and that its concentration is maintained at a comparatively high level by ongoing fusion with endosomes and lysosomes. Being exposed to the cytosolic aspect of the membrane, PS will serve to recruit to the phagosome proteins containing PS-selective C2 domains. Moreover, by conferring onto the phagosomal surface a considerable negative charge, PS will contribute to the recruitment of cationic proteins. The congregation of these proteins on the phagosomal surface likely remodels this organelle and directs its maturation.

Materials and methods

Plasmids

The plasmids encoding GFP-2+, GFP-5+, and GFP-8+ (Roy et al., 2000) were provided by J. Silvius (McGill University, Montreal, Ontario, Canada). GFP-sec61 (Greenfield and High, 1999), GFP-PX (Kanai et al., 2001), and c-Src–GFP (Donepudi and Resh, 2008) were provided by S. High (University of Manchester, Manchester, England, UK), M. Yaffe (Massachusetts Institute of Technology, Cambridge, MA), and M. Resh (Memorial Sloan-Kettering Cancer Center, New York, NY), respectively. Construction of the plasmids encoding mRFP-Palm (Yeung et al., 2006b) and GFP-Lact-C2 (Yeung et al., 2008) was described previously. c-Src–mRFP was constructed by digesting c-Src–GFP with XhoI and BamHI and subcloning the excised fragment into the mRFP-N1 vector, which was provided by R. Tsien (University of California, San Diego, La Jolla, CA). mRFP-PX was provided by G. Mallo. mRFP-2FYVE was constructed by digesting GFP-2FVYE with XhoI and BamHI and then subcloning the excised fragment into the mRFP-C1 vector.

Cell culture, transfection, and treatment

RAW264.7 macrophages from American Type Culture Collection were grown as previously described (Yeung et al., 2008). Transient transfection of cDNA plasmids was performed using FuGene HD (Roche) as described previously (Yeung et al., 2008). Where indicated, the cells were treated with 200 nM wortmannin (EMD) for 15 min to inhibit PI 3-kinase.

Synchronous phagocytosis assay

RAW macrophages were grown on circular glass coverslips placed inside 6-well plates. Sheep RBCs (sRBCs) obtained from MP Biomedicals were opsonized with rabbit anti-RBC IgG (MP Biomedicals) as described previously (Botelho et al., 2000). To synchronously initiate phagocytosis, opsonized RBCs were sedimented onto the RAW macrophages by centrifugation for 1 min at 1,000 rpm using a tabletop centrifuge (Beckman Coulter). After rapidly washing nonadherent RBCs, the cells were bathed in Hepes-buffered medium RPMI 1640 (Wisent Inc.), and phagocytosis was allowed to proceed for 1, 5, or 60 min at 37°C. Coverslips were then transferred from the 6-well plate to an Attofluor live cell imaging chamber (Invitrogen) for microscopy. To arrest further phagosome maturation, the cells were bathed in ice-cold Hepes-buffered medium RPMI 1640 during the course of image acquisition. Synchronous phagocytosis of 3-µm latex beads was performed similarly and has been previously described (Yeung et al., 2006b).

L. pneumophila infection protocol

L. pneumophila (strain LpO2) and *L. pneumophila* expressing GFP-*fla*A (MB355; Hammer and Swanson, 1999) were cultured to the postexponential phase in ACES yeast extract broth as described previously (provided by M. Swanson, University of Michigan Medical School, Ann Arbor, MI; Byrne and Swanson, 1998). RAW macrophages were infected with *L. pneumophila* for 2 h at a multiplicity of infection of 10 followed by washing to remove excess bacteria and a further 2–4-h incubation at 37°C. For immunostaining, the infected cells were fixed and permeabilized with cold methanol, blocked with 5% goat serum, and incubated sequentially with rabbit anti–*L. pneumophila* antibody (1:2,000 dilution; provided by R. Isberg, Tufts University, Boston, MA) followed by Cy3-conjugated donkey anti–rabbit antibody (1:1,000; Jackson ImmunoResearch Laboratories).

C. trachomatis infection protocol

Frozen stocks of *C. trachomatis* serotype L2 elementary bodies were prepared as previously described (Tse et al., 2005). For infection, frozen vials containing *C. trachomatis* were thawed, and elementary bodies were added to RAW macrophages grown on coverslips at the bottom of 6-well plates. The plates were spun for 20 min at 2,000 rpm before incubation for 18 h at 37°C. Cells were fixed with 8% PFA (Electron Microscopy Sciences) for 2 h *C. trachomatis* within RAW macrophages were visualized using the fluorescent DNA stain Draq5 as suggested by the manufacturer (Biostatus).

Image acquisition and analysis

All fluorescence images were acquired using a microscope (Axiovert 200M; Carl Zeiss, Inc.) equipped with a 63×/1.40 NA oil immersion lens (Carl Zeiss, Inc.), charge-coupled device camera (C9100-13; Hamamatsu Photonics), and a spinning-disc confocal system (Quorum) as described previously (Yeung et al., 2008). Images were captured and analyzed using Volocity software (PerkinElmer). The ratio of the fluorescence intensity of the phagosome to that of the bulk, unengaged plasma membrane was calculated

as described previously (Yeung et al., 2006b). In brief, regions of interest were defined in the phagosomal membrane, unengaged plasma membrane, and cytosol, and their mean fluorescence intensities were measured. After subtracting the cytosolic contribution, the excess fluorescence associated to the phagosome and bulk membranes was estimated, and their ratio was then calculated. A value of 1 indicates similar probe density at the phagosomal and bulk plasma membrane. A value of 0 indicates complete loss of the probe from the phagosomal membrane. For quantification of Lact-C2 staining of *C. trachomatis*– or *L. pneumophila*–containing vacuoles, the fluorescence associated with the vacuolar membrane was either scored as positive or negative and was reported as the percentage of the total number of vacuoles counted.

Analysis of the lipid selectivity of the anti-PS antibody

Nucleosil 120–3 C18 beads (3 µm; Richard Scientific) coated with PC or PC plus 20% PE, 20% PS, 20% PA, 2% PI, or 2% PI[4,5]P_2 were prepared as described previously (Yeung et al., 2008). Lipid-coated beads were incubated with an Alexa Fluor 488–conjugated mouse anti-PS antibody (Millipore) for 1 h in 20 mM Tris-HCl, pH 7. An FACS scan flow cytometer (BD) was used to analyze fluorescence associated with the beads.

Lipid-binding analysis of annexin-V

Large unilamellar vesicles (LUVs) of dansyl-PE:PC (2:98), dansyl-PE:PC:PE (2:78:20), dansyl-PE:PC:PS (2:78:20), dansyl-PE:PC:PA (2:78:20), dansyl-PE:PC:PG (2:78:20), dansyl-PE:PC:PI(4)P (2:96:2), or dansyl-PE:PC:PI(4,5)P_2 (2:96:2) were prepared using a liposome extruder (Avestin) as described previously (Yeung et al., 2006b). The binding of annexin-V to the LUVs was measured using a fluorescence resonance energy transfer (FRET) assay. In brief, purified human placental annexin-V (Sigma-Aldrich) was added to LUVs suspended in a buffer containing 10 mM Hepes and 100 µM Ca^{2+}, pH 7.4. FRET between the tryptophan residues of annexin-V and the dansylated lipids was recorded using a spectrophotometer (F-2500; Hitachi) with excitation at 280 nm and emission at 505 nm. FRET resulting from binding of annexin to liposomes was measured in the presence and absence of calcium, which is required for annexin binding. The FRET signal observed in the absence of calcium, indicative of nonspecific binding, was subtracted from the signal recorded in the presence of calcium. To facilitate comparison between experiments, the data are normalized to the binding to PC liposomes recorded in the absence of calcium.

Phenotypic assessment of the endocytic pathway in yeast

To assess vacuole acidification in vivo, yeast cells were stained with quinacrine as described previously (Weisman et al., 1987) with minor modifications. In brief, wild-type or PS synthase–deficient (*cho1*) yeast cells grown to the early logarithmic phase were harvested by centrifugation at 2,000 *g* and incubated in YPD (1% yeast extract, 2% peptone, and 2% glucose), pH 7.6, for 30 min. Cells were harvested and resuspended in 50 mM phosphate-buffered saline, pH 7.6, containing 2% glucose, and quinacrine was added to a final concentration of 200 µM to cells. After 5 min, the cells were harvested, resuspended in PBS-2% glucose, and examined immediately by epifluorescence and differential interference contrast microscopy.

To assess the traffic and appearance of the endocytic pathway, a pulse-chase analysis using the lipophilic styryl dye FM4-64 was used as described previously (Vida and Emr, 1995). In brief, cells were grown to early logarithmic phase in YPD medium at 30°C, harvested, and resuspended at 20 OD_{600} U/ml in YPD medium. To pulse the cells with FM4-64, the dye was added to cells at a final concentration of 32 µM from a 16-mM stock in DMSO and incubated at 4°C for 30 min while rotating. The cells were next sedimented, resuspended in YPD medium, and incubated at 30°C for the indicated times. After this chase period, the cells were harvested, resuspended in PBS, placed on ice, and examined microscopically as described in Image acquisition and analysis.

Online supplemental material

Fig. S1 shows an assessment of the surface charge of maturing phagosomes during latex bead phagocytosis. Fig. S2 shows PS and phagosomal membrane charge during *L. pneumophila* and *C. trachomatis* vacuole maturation. Fig. S3 shows lipid-binding specificity of the anti-PS antibody and annexin-V. Fig. S4 shows membrane fusion and fission during phagosomal maturation. Fig. S5 shows phenotypic assessment of the endocytic pathway in wild-type and PS-deficient yeast. Video 1 shows distribution of charge and membrane markers during phagosome formation and maturation. Video 2 shows distribution of PS during phagosome formation and maturation. Online supplemental material is available at http://www.jcb.org/cgi/content/full/jcb.200903020/DC1.

This work was supported by the Canadian Institutes of Health Research (CIHR; grant 7075). T. Yeung is the recipient of a graduate studentship from the CIHR. B. Heit is supported by the Heart and Stroke Foundation of Ontario. G.D. Fairn is the recipient of the CIHR postdoctoral fellowship. J.F. Dubuisson and M. Swanson are supported by the National Institutes of Health (grant 2 R01 AI040694). S. Grinstein is the current holder of the Pitblado Chair in Cell Biology and is cross-appointed to the Department of Biochemistry of the University of Toronto.

Submitted: 5 March 2009
Accepted: 4 May 2009

References

Andersen, M.H., H. Graversen, S.N. Fedosov, T.E. Petersen, and J.T. Rasmussen. 2000. Functional analyses of two cellular binding domains of bovine lactadherin. *Biochemistry.* 39:6200–6206.

Botelho, R.J., M. Teruel, R. Dierckman, R. Anderson, A. Wells, J.D. York, T. Meyer, and S. Grinstein. 2000. Localized biphasic changes in phosphatidylinositol-4,5-bisphosphate at sites of phagocytosis. *J. Cell Biol.* 151:1353–1368.

Brumell, J.H., and M.A. Scidmore. 2007. Manipulation of rab GTPase function by intracellular bacterial pathogens. *Microbiol. Mol. Biol. Rev.* 71:636–652.

Byrne, B., and M.S. Swanson. 1998. Expression of *Legionella pneumophila* virulence traits in response to growth conditions. *Infect. Immun.* 66:3029–3034.

Desjardins, M., J.E. Celis, G. van Meer, H. Dieplinger, A. Jahraus, G. Griffiths, and L.A. Huber. 1994. Molecular characterization of phagosomes. *J. Biol. Chem.* 269:32194–32200.

Donepudi, M., and M.D. Resh. 2008. c-Src trafficking and co-localization with the EGF receptor promotes EGF ligand-independent EGF receptor activation and signaling. *Cell. Signal.* 20:1359–1367.

Gilbert, G.E., and D. Drinkwater. 1993. Specific membrane binding of factor VIII is mediated by O-phospho-L-serine, a moiety of phosphatidylserine. *Biochemistry.* 32:9577–9585.

Gillooly, D.J., A. Simonsen, and H. Stenmark. 2001. Cellular functions of phosphatidylinositol 3-phosphate and FYVE domain proteins. *Biochem. J.* 355:249–258.

Greenfield, J.J., and S. High. 1999. The Sec61 complex is located in both the ER and the ER-Golgi intermediate compartment. *J. Cell Sci.* 112:1477–1486.

Hammer, B.K., and M.S. Swanson. 1999. Co-ordination of *legionella pneumophila* virulence with entry into stationary phase by ppGpp. *Mol. Microbiol.* 33:721–731.

Heo, W.D., T. Inoue, W.S. Park, M.L. Kim, B.O. Park, T.J. Wandless, and T. Meyer. 2006. PI(3,4,5)P3 and PI(4,5)P2 lipids target proteins with polybasic clusters to the plasma membrane. *Science.* 314:1458–1461.

Kanai, F., H. Liu, S.J. Field, H. Akbary, T. Matsuo, G.E. Brown, L.C. Cantley, and M.B. Yaffe. 2001. The PX domains of p47phox and p40phox bind to lipid products of PI(3)K. *Nat. Cell Biol.* 3:675–678.

Leventis, R., and J.R. Silvius. 1998. Lipid-binding characteristics of the polybasic carboxy-terminal sequence of K-ras4B. *Biochemistry.* 37:7640–7648.

Majeed, M., E. Caveggion, C.A. Lowell, and G. Berton. 2001. Role of Src kinases and Syk in Fcgamma receptor-mediated phagocytosis and phagosome-lysosome fusion. *J. Leukoc. Biol.* 70:801–811.

Marshall, J.G., J.W. Booth, V. Stambolic, T. Mak, T. Balla, A.D. Schreiber, T. Meyer, and S. Grinstein. 2001. Restricted accumulation of phosphatidylinositol 3-kinase products in a plasmalemmal subdomain during Fcγ receptor-mediated phagocytosis. *J. Cell Biol.* 153:1369–1380.

McLaughlin, S., and D. Murray. 2005. Plasma membrane phosphoinositide organization by protein electrostatics. *Nature.* 438:605–611.

Niedergang, F., and P. Chavrier. 2004. Signaling and membrane dynamics during phagocytosis: many roads lead to the phagos(R)ome. *Curr. Opin. Cell Biol.* 16:422–428.

Oh, Y.K., and J.A. Swanson. 1996. Different fates of phagocytosed particles after delivery into macrophage lysosomes. *J. Cell Biol.* 132:585–593.

Peyron, P., I. Maridonneau-Parini, and T. Stegmann. 2001. Fusion of human neutrophil phagosomes with lysosomes in vitro: involvement of tyrosine kinases of the Src family and inhibition by mycobacteria. *J. Biol. Chem.* 276:35512–35517.

Pralle, A., P. Keller, E.L. Florin, K. Simons, and J.K. Horber. 2000. Sphingolipid–cholesterol rafts diffuse as small entities in the plasma membrane of mammalian cells. *J. Cell Biol.* 148:997–1008.

Raynal, P., and H.B. Pollard. 1994. Annexins: the problem of assessing the biological role for a gene family of multifunctional calcium- and phospholipid-binding proteins. *Biochim. Biophys. Acta.* 1197:63–93.

Roy, M.O., R. Leventis, and J.R. Silvius. 2000. Mutational and biochemical analysis of plasma membrane targeting mediated by the farnesylated, polybasic carboxy terminus of K-ras4B. *Biochemistry.* 39:8298–8307.

Salcedo, S.P., and D.W. Holden. 2005. Bacterial interactions with the eukaryotic secretory pathway. *Curr. Opin. Microbiol.* 8:92–98.

Shi, J., C.W. Heegaard, J.T. Rasmussen, and G.E. Gilbert. 2004. Lactadherin binds selectively to membranes containing phosphatidyl-L-serine and increased curvature. *Biochim. Biophys. Acta.* 1667:82–90.

Shin, S., and C.R. Roy. 2008. Host cell processes that influence the intracellular survival of *Legionella pneumophila*. *Cell. Microbiol.* 10:1209–1220.

Swanson, J.A., and A.D. Hoppe. 2004. The coordination of signaling during Fc receptor-mediated phagocytosis. *J. Leukoc. Biol.* 76:1093–1103.

Swanson, M.S., and R.R. Isberg. 1995. Association of *Legionella pneumophila* with the macrophage endoplasmic reticulum. *Infect. Immun.* 63:3609–3620.

Tse, S.M., D. Mason, R.J. Botelho, B. Chiu, M. Reyland, K. Hanada, R.D. Inman, and S. Grinstein. 2005. Accumulation of diacylglycerol in the *Chlamydia* inclusion vacuole: possible role in the inhibition of host cell apoptosis. *J. Biol. Chem.* 280:25210–25215.

Vance, J.E., and R. Steenbergen. 2005. Metabolism and functions of phosphatidylserine. *Prog. Lipid Res.* 44:207–234.

Vida, T.A., and S.D. Emr. 1995. A new vital stain for visualizing vacuolar membrane dynamics and endocytosis in yeast. *J. Cell Biol.* 128:779–792.

Vieira, O.V., R.J. Botelho, L. Rameh, S.M. Brachmann, T. Matsuo, H.W. Davidson, A. Schreiber, J.M. Backer, L.C. Cantley, and S. Grinstein. 2001. Distinct roles of class I and class III phosphatidylinositol 3-kinases in phagosome formation and maturation. *J. Cell Biol.* 155:19–25.

Weisman, L.S., R. Bacallao, and W. Wickner. 1987. Multiple methods of visualizing the yeast vacuole permit evaluation of its morphology and inheritance during the cell cycle. *J. Cell Biol.* 105:1539–1547.

Yeung, T., G.E. Gilbert, J. Shi, J. Silvius, A. Kapus, and S. Grinstein. 2008. Membrane phosphatidylserine regulates surface charge and protein localization. *Science.* 319:210–213.

Yeung, T., B. Ozdamar, P. Paroutis, and S. Grinstein. 2006a. Lipid metabolism and dynamics during phagocytosis. *Curr. Opin. Cell Biol.* 18:429–437.

Yeung, T., M. Terebiznik, L. Yu, J. Silvius, W.M. Abidi, M. Philips, T. Levine, A. Kapus, and S. Grinstein. 2006b. Receptor activation alters inner surface potential during phagocytosis. *Science.* 313:347–351.